Hindawi
Advances in Astronomy
Volume 2019, Article ID 3641204, 9 pages
https://doi.org/10.1155/2019/3641204

Research Article

Revisiting the Question: The Cause of the Solar Cycle Variation of Total Solar Irradiance

N. B. Xiang [1,2]

[1] *Yunnan Observatories, Chinese Academy of Sciences, Kunming 650011, China*
[2] *State Key Laboratory of Space Weather, Chinese Academy of Sciences, Beijing 100190, China*

Correspondence should be addressed to N. B. Xiang; nanbin@ynao.ac.cn

Received 14 November 2018; Revised 1 February 2019; Accepted 5 March 2019; Published 26 March 2019

Academic Editor: Geza Kovacs

The Mg II index and sunspot area are usually used to represent the intensification contribution by solar bright structures to total solar irradiance (TSI) and sunspot darkening, respectively. In order to understand the cause of the solar cycle variation of TSI, we use extension of wavelet transform, wavelet coherence (WTC), and partial wavelet coherence (PWC), to revisit this issue. The WTC of TSI with sunspot area shows that the two time series are very coherent on timescales of one solar cycle, but the PWC of TSI with sunspot area, which can find the results of WTC after eliminating the effect of the Mg II index, indicates that the solar cycle variation of TSI is not related to sunspots on the solar surface. The coherence of two time series at these timescales should be due to a particular phase relation between sunspots and TSI. The WTC and PWC of TSI with Mg II index show that the solar cycle variation of TSI is highly related to Mg II index, which reflects the relation of TSI with the long-term part of Mg II index that shows the intensification contribution by the small magnetic features to TSI. Consequently, the solar cycle variation of TSI is dominated by the small magnetic features on the solar full disk. Additionally, we also show the combined effects of the sunspot darkening and the intensification contribution represented by Mg II index to TSI on timescales of a few days to several months and indicate that the faculae increase TSI and contribute to its variation at these timescales.

1. Introduction

The total solar irradiance (TSI) is the total solar electromagnetic energy flux over the whole spectrum which arrives at the top of the Earth's atmosphere at the mean Sun-Earth distance. Apart from its important role in helping us understand the Sun, TSI controls the total energy from the Sun into the Earth system, which drives almost every known physical and biological cycle in Earth system. The variation in TSI is one of the most key factors which affects the Earth's climate, and so it is also one of the important factors which affects the living environment of mankind. Thus, there are many studies on this topic [1–5].

The TSI was first measured by radiometer on board satellites in October 1978, and space-based measurements have continued for more than 40 years. The satellite measurements near Earth show that the TSI varies at all of the timescales it is measured; that is, it varies from solar minimum to maximum, and from one cycle to the next [6–16]. It is generally accepted that the variations of TSI on timescales of minutes to hours are mainly related to granulation, mesogranulation, and supergranulation [17], and the variations in TSI on timescales of a few days to weeks are dominated by the evolution of magnetic features on the solar surface [12, 17, 18]. However, the variation of TSI on timescales of one solar cycle is still an open issue. The early studies indicated that the variations of TSI at these timescales are mainly due to the combination of the sunspots blocking and the intensification due to bright faculae, plages, and network elements [19–21]. But Li et al. [14] proposed that the solar cycle variation of TSI should be dominated by the network magnetic elements in quiet regions. Fröhlich [9] advised that the solar cycle variation of TSI is probably due to a change of the global temperature of the Sun modulated by the strength of activity but not modulated by the surface magnetism as the solar cycle modulation. Xiang and Kong [15] investigated the relation between TSI and magnetic fields and found that the weak magnetic activity seen on the solar full disk dominates the

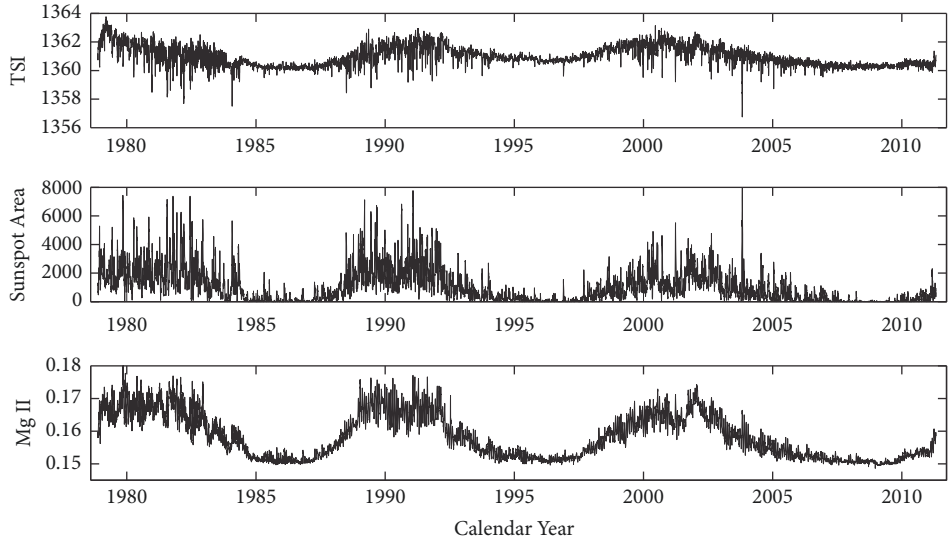

Figure 1: The three solar indices: daily ACRIM TSI (top panel), daily sunspot area (middle panel), and daily Mg II core-to-wing ratio (bottom panel) from 1978 November 17 to 2011 April 29.

solar cycle variation of TSI. This result is the same as the finding in Li et al. [22], in which the conclusion is based on the phase relations between TSI and Mg II core-to-wing ratio. Recently, Xu et al. [16] studied the phase relations between TSI and sunspot number and indicated that TSI and sunspot number are very coherent, which hints that the solar cycle variation of TSI should be dominated by the solar activity regions. It is well known that the Sun brightening increases TSI and the darkening decreases it, and TSI is a global parameter averaged over the solar disk. Just based on the discussion of the phase relations between TSI and sunspot number, the results are not convincing. Revisiting this topic is of significance and is needed.

On the other hand, there are several models which can reconstruct TSI, and the most successful model of reconstruction of TSI should be the SATIRE model, which assumes that the irradiance variations should be entirely caused by the evolution of the solar surface magnetic field on timescales of half a day to one Schwabe solar cycle [23–27]. The SATIRE model divided the solar surface features into four types: the quiet sun, sunspot umbrae, sunspot penumbrae, and faculae/network [24, 25]. Thus, according to the SATIRE model and the current theories, the darkening and brightening effect are the main reasons to cause the variations of TSI, although the variations are not completely caused by them. It is difficult to directly measure the sunspots blocking and the intensification due to bright faculae, plages, and network elements; the best way is to choose proxies which can describe the sunspots blocking or the intensification of bright faculae, plages, and network elements, such as sunspot number or areas, which can describe sunspot darkening, and facular areas, Ca II or Mg II indices, which can describe the intensification of solar bright structures [9, 11, 28–31]. Moreover, it is known that the Mg II index can be separated into a short-term and long-term part. The short-term part indicates that the facular intensifies TSI, and the long-term part shows the intensification contribution by the small magnetic features to TSI [9, 12, 22]. Consequently, we use sunspot area and Mg II index and combine extension of wavelet transform to revisit the reason for the solar cycle variation of TSI.

2. The Reason for the Solar Cycle Variation of TSI

Three time series in our study are as follows.

The first is New Active Cavity Radiometer Irradiance Monitoring (ACRIM) TSI. Currently, there are three TSI composites: Physikalisch Meteorologisches Observatorium Davos (PMOD) TSI [7, 28], ACRIM TSI [32–34], and Royal Meteorological Institute of Belgium (RMIB) TSI [35, 36]. We do not discuss the difference among the three TSI composites. According to the Total Irradiance Monitor (TIM) and a series of new radiometric laboratory observations, the most probable value of TSI representative of solar minimum is 1360.8±0.5 W m^2, lower than the canonical value of 1365.4±1.3 W m^2 recommended a decade ago [13]. It looks like ACRIM TSI and RMIB TSI may be closer to the observation values than PMOD TSI, but RMIB TSI is not available online. Moreover, the new ACRIM TSI is recalibrated with updated sensor degradation and algorithm LAPS/TRF corrections for scattering, diffraction, and TSI scale, and the data during ACRIM gap is recalibrated as well [34]. Thus, only ACRIM TSI is used in this study. Figure 1 (top panel) shows the daily ACRIM TSI composite from 1978 November 17 to 2011 April 29, which can be downloaded from the website http://www.acrim.com/Data%20Products.htm.

The second is daily sunspot area of the full Sun. Sunspot area is sometimes used to represent "the sunspots blocking" [11, 37], which can be downloaded from NASA

(https://solarscience.msfc.nasa.gov/greenwch.shtml).

Figure 1 (middle panel) shows daily sunspot area in the same time interval.

The third is Mg II core-to-wing ratio, called Mg II index in this study, which is a robust measure of chromospheric activity [38–40]. The core is formed in the upper chromosphere, where the temperature is about 7000K, but the broad wings are from the upper photosphere. The variability of the photosphere (wings) is quite small, while the chromospheric activity causes about 30% variations of the core. Because the core-to-wing ratio is not easily affected by the instruments, Mg II index which is used to represent "the intensification due to bright faculae, plages, and network elements" is very reliable [11, 37, 38]. The Mg II index composite can be downloaded from the website http://www.iup.uni-bremen.de/gome/gomemgii.html. Figure 1 (bottom panel) shows the Mg II index in the same time interval.

2.1. Method. The wavelet analysis is widely used to analyze the nonstationary signals and the evolution in time of each periodic oscillation [41, 42]. Generally, the wavelet transform expands time series into time frequency space and thus is a powerful tool for analyzing localized intermittent oscillations in a time series [41–45]. In astronomic studies, we often hope to examine two series together which should be linked in some way, which are suggestive of causality between two time series. The extension of wavelet transform, wavelet coherence (WTC), is widely used to find significant coherence between two time series even though the common power is low, and the results from WTC can be thought of the local correlation between two time series in time-frequency space; thus WTC is a powerful method for testing proposed linkages between two time series [16, 42, 46] and is also particularly useful for investigating the relation of TSI with sunspot area and Mg II index in this study. The WTC of two time series $X_n, n = 1, \ldots, N$ and $Y_n, n = 1, \ldots, N$ is defined as [42, 46]:

$$R_n^2(s) = \frac{\left|S\left(s^{-1}W_n^{XY}(s)\right)\right|^2}{S\left(s^{-1}\left|W_n^X(s)\right|^2\right)\cdot S\left(s^{-1}\left|W_n^Y(s)\right|^2\right)} \quad (1)$$

where $W_n^X(s)$ is the wavelet transform of time series X_n, and it is represented as $W_n^X(s) = \sqrt{\delta t/s}\,\Sigma_{n'=1}^{N} X_{n'}\Psi_0[(n' - n)\delta t/s]$. There, δt and Ψ_0 indicate the uniform time step and wavelet basis selected in the wavelet transform, respectively; accordingly, s indicates the variational scale of wavelet when the wavelet is stretched in time. Moreover, the Morlet wavelet, $\Psi_0(\eta) = \pi^{-1/4}e^{i\omega_0\eta}e^{(-1/2)\eta^2}$, is selected in this study, where ω_0 is dimensionless frequency ($\omega_0 = 6$), and η is dimensionless time. Similarly, $W_n^Y(s)$ shown in function (1) is the wavelet transform of time series Y_n. $W_n^{XY}(s)$ displays the cross-wavelet transform of two time series X_n and Y_n, and it can be defined as $W^{XY} = W^X W^{Y*}$, where * denotes complex conjugation. Finally, S displayed in function (1) is a smoothing operator. It looks like the definition of the WTC closely resembles a tradition correlation coefficient. The smoothing operator S can be written as the function

$$S(W) = S_{scale}\left(S_{time}\left(W_n(s)\right)\right) \quad (2)$$

where S_{scale} denotes smoothing along the wavelet scale axis, and S_{time} denotes smoothing in time. The Morlet wavelet is used in this study, and so a suitable smoothing operator is given as the following functions [42, 46]:

$$S_{time}(W)\big|_s = \left(W_n(s) * c_1^{-t^2/2s^2}\right)\Big|_s \quad (3)$$

$$S_{scale}(W)\big|_n = \left(W_n(s) * c_2\prod(0.6s)\right)\Big|_n \quad (4)$$

where c_1 & c_2 are normalization constants and $\prod$ is the rectangle function. For the Morlet wavelet, the factor 0.6 in function (4) is the empirically determined scale decorrelation length [41, 42, 46]. In practice, both convolutions are done discretely; therefore the normalization coefficients are determined numerically. Finally, the Monte Carlo method is used to assess the statistical significance level of the WTC against red noise backgrounds [42, 46]. Consequently, the WTC is a tool for identifying possible relationships and revealing intermittent correlations between two time series.

The WTC can be used to find significant coherence regions and analyze the relations of TSI with sunspot area and Mg II index on timescales of a few days to one Schwabe solar cycle. But there are some shortages, since the WTC is based on a bivariate analysis. For instance, when we study the relation of TSI with sunspot area, the "stand-alone" relationship between TSI and sunspot area should be studied after eliminating the effect of Mg II index; hence we need a trivariate algorithm to validate the results of WTC analysis after eliminating the effect of Mg II index.

In probability theory and statistics, the partial correlation can be used to estimate the degree of association between two random variables, with the effect of a set of controlling random variables removed. Partial wavelet coherence (PWC) is a technique similar to partial correlation that is utilized to find the results of WTC between two time series y and x_1 after eliminating the effect of the time series x_2 [47, 48]. The PWC squared of two time series y and x_1 (after eliminating the effect of the time series x_2) can be defined as the following function [47, 49]:

$$RP^2(y, x_1, x_2) = \frac{\left|R(y, x_1) - R(y, x_2)\cdot R(y, x_1)^*\right|^2}{\left[1 - R(y, x_2)\right]^2\left[1 - R(x_2, x_1)\right]^2} \quad (5)$$

which is similar to the simple WTC, ranging from 0 to 1. In practice, the WTC analysis of time series y and x_1 shows a high squared at particular time-frequency space but where a low $RP^2(y, x_1, x_2)$ was found; we still can imply that the time series x_1 does not have a significant effect on the time series y at that particular time-frequency space. If the WTC of time series y and x_1 and the WTC of time series y and x_2 display the same significant bands at particular time-frequency space where both $RP^2(y, x_1, x_2)$ and $PR^2(y, x_2, x_1)$ also have the same significant bands, both x_1 and x_2 have a significant influence on y at that particular time-frequency space. Additionally, the statistical significance level of the PWC is estimated by using Monte Carlo method [47]. In this study, the WTC (codes provided by Grinsted et al. [42]) is used to investigate the relation of ACRIM TSI with sunspot area and Mg II index, respectively. Then we use the PWC (codes provided by Ng and Chan [47]) to find the results of

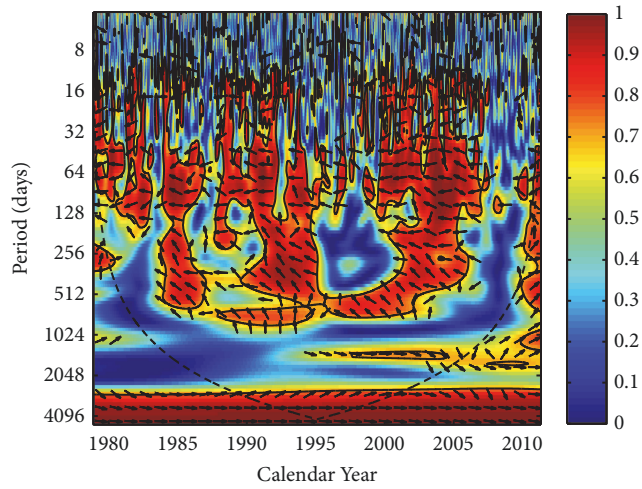

Figure 2: Wavelet coherence of the daily TSI and sunspot area. The dashed black line indicates the COI where edge effects might distort the picture, and the 95% confidence level is shown as a thick contour, which is estimated by Monte Carlo method. The relative phase relation is shown as arrows (with in-phase pointing right, antiphase pointing left, and TSI leading sunspot area by 90° pointing straight down).

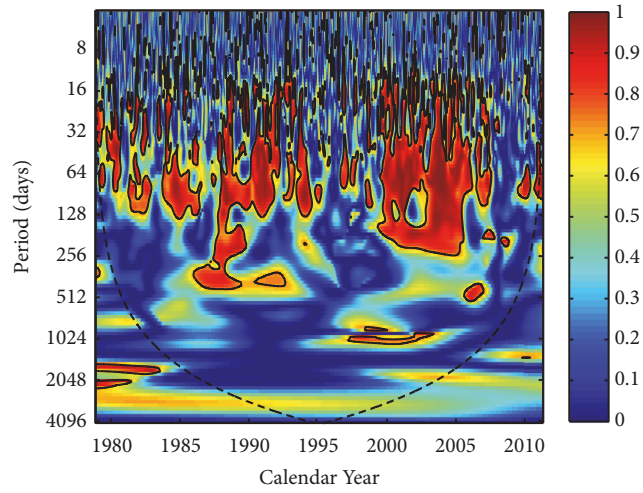

Figure 3: Partial wavelet coherence of the daily TSI and sunspot area (after eliminating the effect of Mg II index). The dashed black line indicates the COI where edge effects might distort the picture, and the 95% confidence level is shown as a thick contour, which is estimated by Monte Carlo method.

the WTC analysis and to try to revisit the reason that causes the solar cycle variation of TSI.

2.2. Data Analysis. TSI, sunspot area, and Mg II index are systematically observed, but some days do not have observations. In order to use the WTC and PWC to analyze the relation of TSI with sunspot area and Mg II index, the cubic spline interpolation is used to interpolate the values when these days do not have observation records in three time series. The WTC spectrum of TSI and sunspot area is shown in Figure 2, which can be thought of the local correlations between TSI and sunspot area. The PWC spectrum of TSI and sunspot area is shown in Figure 3, which can find the results of WTC between TSI and sunspot area (after eliminating the effect of Mg II index). In high frequency band, many small intermittent common power regions of above 95% confidence level are shown on timescales of a few days to one solar rotation cycle in Figure 2. Moreover, there are large continuous common power regions of above 95% confidence level on timescales of one solar rotation cycle to one year in this figure, where the arrows almost point to left or left and above. In Figure 3, it can be found that many intermittent common power regions and large continuous region of above the 95% confidence level are also shown on timescales of a few days to several months from 1978 November to 2011 April. Combining Figures 2 and 3, we can infer that the variations of TSI should be related to sunspot area on timescales of a few days to several months. The relative phase relation shown as arrows indicates that the sunspots decrease TSI. Though this result coincides with earlier papers [12, 17, 18, 50], at least we use other methods to directly confirm the previous results. We also compare TSI and sunspot area in two discretional

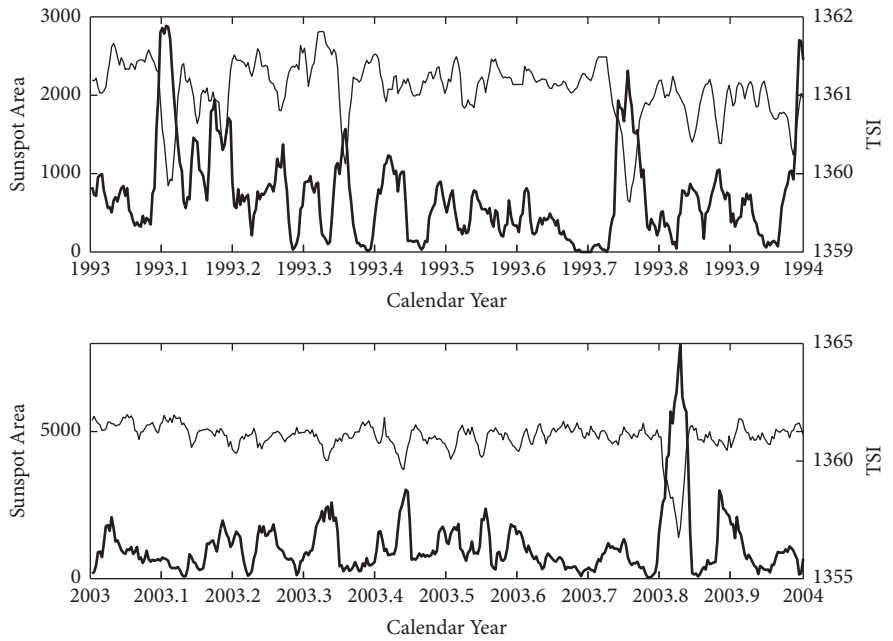

Figure 4: Comparison of TSI (the thin line) and sunspot area (the thick line) in the years 1993 (the top panel) and 2003 (the bottom panel), respectively.

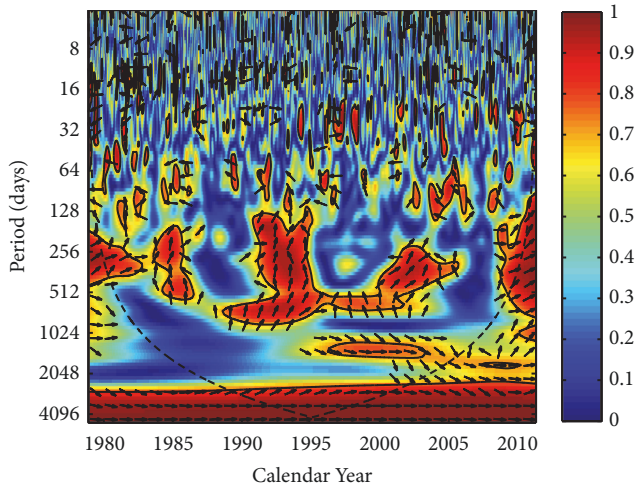

Figure 5: Wavelet coherence of the daily TSI and Mg II index. The dashed black line indicates the COI where edge effects might distort the picture, and the 95% confidence level is shown as a thick contour, which is estimated by Monte Carlo method. The relative phase relation is shown as arrows (with in-phase pointing right, antiphase pointing left, and TSI leading Mg II index by 90° pointing straight down).

years (1993 and 2003), and the results are shown in Figure 4, which indicate that the variations of TSI are sometimes not caused by sunspot area at short timescales. In low frequency band, a continuous power region of above 95% confidence level is shown in Figure 2 on timescales of one Schwabe solar cycle. However, the PWC shows that the power is very low at these timescales, and there is no region of above 95% confidence level in Figure 3. Combining the WTC and PWC, we can infer that the solar cycle variation of TSI should not be related to sunspot area.

Using the same methods, we analyze the relation of TSI with Mg II index. The WTC and PWC spectra of TSI and Mg II index are shown in Figures 5 and 6, respectively. In high frequency band, the WTC spectrum of TSI and Mg II index (Figure 5) shows there are many intermittent small regions of above 95% confidence level on timescales of a few days to several months. Figure 6 is utilized to find the results of the WTC between the TSI and Mg II index (after eliminating the effect of sunspot area). It can be found that many intermittent small regions of above 95% confidence level are also shown on timescales of a few days to several months. Combining Figures 5 and 6, it is inferred that the variations of TSI should be related to Mg II index on timescales of a few days to several months. That is to say, the intensification of solar bright

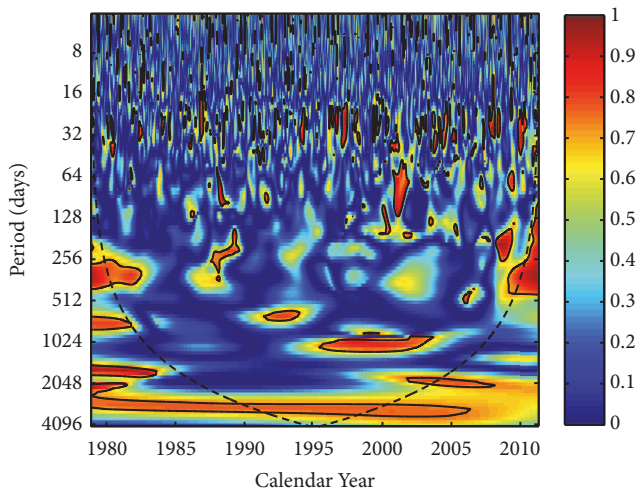

Figure 6: Partial wavelet coherence of the daily TSI and Mg II index (after eliminating the effect of sunspot area). The dashed black line indicates the COI where edge effects might distort the picture, and the 95% confidence level is shown as a thick contour, which is estimated by Monte Carlo method.

structures, which is represented by Mg II index, increases TSI and contributes to its variation at these timescales. This result is the same as earlier papers as well [12, 17, 18, 51]. In low frequency band, a continuous common power region of above 95% confidence level is shown in Figure 5 on timescales of one Schwabe solar cycle. Moreover, the PWC spectrum of TSI and Mg II index (Figure 6) also shows there is a common significant region of above 95% confidence level at these timescales. Combining the WTC and PWC, we infer that the solar cycle variation of TSI is probably highly related to Mg II index.

3. Conclusions and Discussion

In order to revisit the controversial topic in recent literatures: what causes the solar cycle variation of TSI? The WTC and PWC are used to study this topic. Used in this study are daily TSI, daily sunspot area, and daily Mg II index from 1978 November 17 to 2011 April 29.

Figures 2 and 3 show that the sunspots decrease TSI on timescales of a few days to several months. Spruit [52] indicated that the solar convective envelope likes a "thermal superconductor" with a huge thermal inertia, and the same thermal inertia makes possible the irradiance fluctuations due to "superficial" photospheric magnetic structures. Subsequently, a series of studies also indicated that solar irradiance is modulated by photospheric magnetic activity, and the influence of magnetic activity on the solar irradiance varies strongly with the size of the magnetic feature [4, 12, 53]. When sunspots (strong magnetic structures) pass across the visible disk, these strong magnetic structures darken the solar surface and block the energy transportation from the solar interior toward the solar surface, reducing TSI as thermal "plugs [12, 54], since the kilogauss-strength magnetic filed in sunspots is strong enough to largely quench overturning convection [4, 55]. Many papers and our study thus find that the sunspots (strong solar magnetic structures) decrease TSI on timescales of a few days to several months. On the other hand, Figures 5 and 6 indicate that the intensification of solar bright structures, which is represented by Mg II index, increases TSI and contributes to its variation on timescales of a few days to several months. It is known that the Mg II index can be separated into a short-term and long-term part, and the short-term part shows the main intensification contribution of faculae to TSI [9, 12]. Thus, the relation of TSI with Mg II index on timescales of a few days to several months should mainly reflect that of TSI with the short-term part of Mg II index and indicates that the faculae increase TSI and contribute to its variation at short timescales. The combined effects of the sunspots darkening and the intensification of faculae (the short-term part of the Mg II index) to TSI on timescales of one year have been discussed by Li et al. [22]

The results of the WTC and PWC of TSI with the sunspot area shown in Figures 2 and 3 indicate that the solar cycle variation of TSI is not probably related to the sunspots blocking, which is represented by sunspot area. Xu et al. [16] pointed out that TSI is positively correlated with sunspot numbers, the former lags behind the latter by about a solar rotation period, and TSI and sunspot numbers are very coherent on timescales of one Schwabe solar cycle. This hints that the solar cycle variation of TSI should be related to the sunspots (strong magnetic structures) on the solar surface. Li et al. [56] also found that TSI lags behind sunspot activity by about one month. However, the coherence of TSI and sunspot activity on timescales of one solar cycle displayed in Xu et al. [16], which is also shown in Figure 2, should be due to a particular phase relation between sunspots and TSI, but the phase relation of two time series does not indicate that the solar cycle variation of TSI is related to sunspot activity, since the cross-correlation analysis and WTC are based on a bivariate analysis, while the variations of TSI show complicated relations with the solar magnetic activity, and different sizes of the magnetic feature affect TSI in different ways. The results of PWC analysis (Figure 3), which is a

trivariate algorithm and can find the results of the WTC between TSI and sunspot area (after eliminating the effect of the Mg II index), give evidence that the solar cycle variation of TSI is not related to sunspots on the solar surface.

The results of the WTC and PWC of TSI with Mg II index shown in Figures 5 and 6 display that the solar cycle variation of TSI is probably highly related to the intensification contribution, which is represented by Mg II index. Li et al. [22] show that the relation of TSI with Mg II index on timescales of one solar cycle should basically reflect that of the long-term part of Mg II index with TSI; thus the relation of TSI with Mg II index shown in low frequency band of Figures 5 and 6 should mainly reflect that of TSI with the long-term part of Mg II index on timescales of one solar cycle. Moreover, the long-term part of the Mg II index shows the small magnetic features contribution to the intensification of TSI [9, 12]. Consequently, our finding validates that the solar cycle variation of TSI is dominated by the small magnetic features on the solar full disk, which somewhat coincides with early studies [12, 14, 15]. It is known that the small-scale magnetic elements, which populate (and form) the faculae in active regions and quiet Sun network/internetwork [57–59], are bright and raise the energy transportation from the solar interior toward the solar surface, since the darkness is overcome by the lateral heating in the small-scale magnetic concentrations [4, 53, 60–62]. Furthermore, the small magnetic features, which correspond to the faculae in active regions and quiet Sun network/internetwork, present solar cycle variation; thus the intensification contribution of small magnetic features on the full solar disk also displays solar cycle variation and dominates the solar cycle variation of TSI.

In general, the solar magnetic field is distributed over the full solar disk, and the magnetic activity of different sizes and strengths affects TSI in different ways, though the variations of TSI are presently believed to be caused by solar magnetic activity. Relationships among darkening, brightening, and TSI should be very complicated. Moreover, the bright elements on the Sun include mixed network, unipolar network, ephemeral active regions, and polar faculae. The Mg II index used in this study can describe the intensification of solar bright structures, but it is unable to distinguish between these contributions. Consequently, other data, such as faculae and magnetic flux of quiet regions, can be used to further investigate this topic, and it will be the next study focus.

Data Availability

The daily ACRIM TSI can be downloaded from the website http://www.acrim.com/Data%20Products.htm. The daily sunspot area of the full Sun can be found at https://solarscience.msfc.nasa.gov/greenwch.shtml. The Mg II index can be downloaded from the website http://www.iup.uni-bremen.de/gome/gomemgii.html.

Conflicts of Interest

The authors declare that there are no conflicts of interest regarding the publication of this paper.

Acknowledgments

We thank the editor and anonymous referee for their careful reading of the manuscript and for constructive comments that improved the original version. We also thank ACRIM science team for making the TSI composite. This work is supported by the National Natural Science Foundation of China (11573065, 11633008, and 11603069), project supported by the Specialized Research Fund for State Key Laboratories, and the Chinese Academy of Sciences.

References

[1] J. A. Eddy, "The maunder minimum," *Science*, vol. 192, no. 4245, pp. 1189–1202, 1976.

[2] J. D. Haigh, "Climate: climate variability and the influence of the sun," *Science*, vol. 294, no. 5549, pp. 2109–2111, 2001.

[3] T. Egorova, E. Rozanov, V. Zubov, W. Schmutz, and T. Peter, "Influence of solar 11-year variability on chemical composition of the stratosphere and mesosphere simulated with a chemistry-climate model," *Advances in Space Research*, vol. 35, no. 3, pp. 451–457, 2005.

[4] S. K. Solanki, N. A. Krivova, and J. D. Haigh, "Solar irradiance variability and climate," *Annual Review of Astronomy and Astrophysics*, vol. 51, pp. 311–351, 2013.

[5] W. Soon and D. R. Legates, "Solar irradiance modulation of Equator-to-Pole (Arctic) temperature gradients: empirical evidence for climate variation on multi-decadal timescales," *Journal of Atmospheric and Solar-Terrestrial Physics*, vol. 93, pp. 45–56, 2013.

[6] R. C. Willson and H. S. Hudson, "The Sun's luminosity over a complete solar cycle," *Nature*, vol. 351, no. 6321, pp. 42–44, 1991.

[7] C. Fröhlich, "Solar irradiance variability since 1978: revision of the PMOD composite during solar cycle 21," *Space Science Reviews*, vol. 125, no. 1-4, pp. 53–65, 2006.

[8] C. Fröhlich, "Evidence of a long-term trend in total solar irradiance," *Astronomy & Astrophysics*, vol. 501, no. 3, pp. L27–L30, 2009.

[9] C. Fröhlich, "Total solar irradiance: what have we learned from the last three cycles and the recent minimum?" *Space Science Reviews*, vol. 176, no. 1-4, pp. 237–252, 2013.

[10] T. Wenzler, S. K. Solanki, N. A. Krivova, and C. Fröhlich, "Reconstruction of solar irradiance variations in cycles 21-23 based on surface magnetic fields," *Astronomy & Astrophysics* , vol. 460, no. 2, pp. 583–595, 2006.

[11] N. A. Krivova and S. K. Solanki, "Models of solar irradiance variations: current status," *International Journal of Astronomy and Astrophysics*, vol. 29, no. 1-2, pp. 151–158, 2008.

[12] V. Domingo, I. Ermolli, P. Fox et al., "Solar surface magnetism and irradiance on time scales from days to the 11-year cycle," *Space Science Reviews*, vol. 145, no. 3-4, pp. 337–380, 2009.

[13] G. Kopp and J. L. Lean, "A new , lower value of total solar irradiance: evidence and climate significance," *Geophysical Research Letters*, vol. 38, no. 1, 2011.

[14] K. J. Li, W. Feng, J. C. Xu et al., "Why is the solar constant not a constant?" *The Astrophysical Journal*, vol. 747, no. 2, article 135, 5 pages, 2012.

[15] N. B. Xiang and D. F. Kong, "What causes the inter-solar-cycle variation of total solar irradiance?" *The Astronomical Journal*, vol. 150, article 171, 8 pages, 2015.

[16] J. C. Xu, J. L. Xie, and Z. N. Qu, "Phase relations between the sunspot numbers and total solar irradiance," *The Astrophysical Journal*, vol. 851, no. 2, article 141, 9 pages, 2017.

[17] S. K. Solanki, A. D. Seleznyov, and N. A. Krivova, "Solar irradiance fluctuations on short timescales," *Solar Variability as an Input to the Earth's Environment*, vol. 535, pp. 285–288, 2003.

[18] G. L. Withbroe, "Sources of solar total irradiance variations," *Solar Physics*, vol. 257, no. 1, pp. 71–81, 2009.

[19] J. Pap, W. K. Tobiska, and S. D. Bouwer, "Periodicities of solar irradiance and solar activity indices, I," *Solar Physics*, vol. 129, no. 1, pp. 165–189, 1990.

[20] R. B. Lee, M. A. Gibson, R. S. Wilson, and S. Thomas, "Long-term total solar irradiance variability during sunspot cycle 22," *Journal of Geophysical Research*, vol. 100, pp. 1667–1675, 1995.

[21] J. Fontenla, O. R. White, P. A. Fox, E. H. Avrett, and R. L. Kurucz, "Calculation of solar irradiances. i. synthesis of the solar spectrum," *The Astrophysical Journal*, vol. 518, no. 1, pp. 480–499, 1999.

[22] K. J. Li, J. C. Xu, N. B. Xiang, and W. Feng, "Phase relations between total solar irradiance and the Mg II index," *Advances in Space Research*, vol. 57, p. 408, 2016.

[23] M. Fligge, S. K. Solanki, and Y. C. Unruh, "Modelling irradiance variations from the surface distribution of the solar magnetic field," *Astronomy & Astrophysics* , vol. 353, no. 1, pp. 380–388, 2000.

[24] N. A. Krivova, S. K. Solanki, M. Fligge, and Y. C. Unruh, "Reconstruction of solar irradiance variations in cycle 23: Is solar surface magnetism the cause?" *Astronomy & Astrophysics* , vol. 399, no. 1, pp. L1–L4, 2003.

[25] N. A. Krivova, S. K. Solanki, and W. Schmutz, "Solar total irradiance in cycle 23," *Astronomy & Astrophysics*, vol. 529, article A81, 6 pages, 2011.

[26] S. K. Solanki, N. A. Krivova, and T. Wenzler, "Irradiance models," *Advances in Space Research*, vol. 35, no. 3, pp. 376–383, 2005.

[27] Y. C. Unruh, N. A. Krivova, S. K. Solanki, J. W. Harder, and G. Kopp, "Spectral irradiance variations: comparison between observations and the SATIRE model on solar rotation time scales," *Astronomy & Astrophysics*, vol. 486, no. 1, pp. 311–323, 2008.

[28] C. Fröhlich and J. Lean, "The Sun's total irradiance: cycles, trends and related climate change uncertainties since 1976," *Geophysical Research Letters*, vol. 25, no. 23, pp. 4377–4380, 1999.

[29] D. G. Preminger, S. R. Walton, and G. A. Chapman, "Photometric quantities for solar irradiance modeling," *Journal of Geophysical Research (Space Physics)*, vol. 107, p. 1354, 2002.

[30] K. Jain and S. S. Hasan, "Modulation in the solar irradiance due to surface magnetism during cycles 21, 22 and 23," *Astronomy & Astrophysics* , vol. 425, no. 1, pp. 301–307, 2004.

[31] R. Kariyappa and K. R. Sivaraman, "Variability of caIi K emission flux over the solar cycle," *Bulletin of the Astronomical Society of India*, vol. 33, pp. 365-365, 2005.

[32] R. C. Willson, "Total solar irradiance trend during solar cycles 21 and 22," *Science*, vol. 277, no. 5334, pp. 1963–1965, 1997.

[33] R. C. Willson and A. V. Mordvinov, "Secular total solar irradiance trend during solar cycles 21-23, 30," *Geophysical Research Letters*, vol. 30, no. 5, p. 1199, 2003.

[34] R. C. Willson, "ACRIM3 and the total solar irradiance database," *Astrophysics and Space Science*, vol. 352, no. 2, pp. 341–352, 2014.

[35] S. Dewitte, D. Crommelynck, and A. Joukoff, "Total solar irradiance observations from DIARAD/VIRGO," *Journal of Geophysical Research: Space Physics*, vol. 109, no. 2, 2004.

[36] S. Mekaoui and S. Dewitte, "Total solar irradiance measurement and modelling during cycle 23," *Solar Physics*, vol. 247, no. 1, pp. 203–216, 2008.

[37] M. Haberreiter, "Mechanisms for total and spectral solar irradiance variations," *Proceedings of the International Astronomical Union*, vol. 5, no. S264, pp. 231–240, 2009.

[38] R. A. Viereck and L. C. Puga, "The NOAA Mg II core-to-wing solar index: construction of a 20-year time series of chromospheric variability from multiple satellites," *Journal of Geophysical Research: Space Physics*, vol. 104, no. 5, pp. 9995–10006, 1999.

[39] R. Viereck, L. Puga, D. McMullin, D. Judge, M. Weber, and W. K. Tobiska, "The Mg II index: A proxy for solar EUV," *Geophysical Research Letters*, vol. 28, no. 7, pp. 1343–1346, 2001.

[40] R. A. Viereck, L. E. Floyd, P. C. Crane et al., "A composite Mg II index spanning from 1978 to 2003," *Space Weather*, vol. 2, no. 10, 2004.

[41] C. Torrence and G. P. Compo, "A practical guide to wavelet analysis," *Bulletin of the American Meteorological Society*, vol. 79, no. 1, pp. 61–78, 1998.

[42] A. Grinsted, J. C. Moore, and S. Jevrejeva, "Application of the cross wavelet transform and wavelet coherence to geophysical times series," *Nonlinear Processes in Geophysics*, vol. 11, no. 5-6, pp. 561–566, 2004.

[43] K. J. Li, P. X. Gao, and T. W. Su, "The schwabe and gleissberg periods in the wolf sunspot numbers and the group sunspot numbers," *Solar Physics*, vol. 229, no. 1, pp. 181–198, 2005.

[44] L. Deng, Z. Qu, G. Dun, and C. Xu, "Phase relationship between polar faculae and sunspot numbers revisited: Wavelet transform analyses," *Publications of the Astronomical Society of Japan*, vol. 65, article 11, 7 pages, 2013.

[45] J. L. Xie, X. J. Shi, and J. Zhang, "Temporal variation of solar coronal rotation," *The Astrophysical Journal*, vol. 841, no. 1, article 42, 6 pages, 2017.

[46] K. J. Li, P. X. Gao, and L. S. Zhan, "Synchronization of hemispheric sunspot activity revisited: Wavelet transform analyses," *The Astrophysical Journal* , vol. 691, no. 1, pp. 537–546, 2009.

[47] E. K. W. Ng and J. C. L. Chan, "Geophysical applications of partial wavelet coherence and multiple wavelet coherence," *Journal of Atmospheric and Oceanic Technology*, vol. 29, no. 12, pp. 1845–1853, 2012.

[48] N. B. Xiang and Z. N. Qu, "Evolutionary characteristics of the interplanetary magnetic field intensity," *The Astronomical Journal*, vol. 156, no. 4, article 152, 11 pages, 2018.

[49] H. Mihanovic', M. Orlic', and Z. Pasaric', "Diurnal thermocline oscillations driven by tidal flow around an island in the Middle Adriatic," *Journal of Marine Systems*, vol. 78, pp. S157–S168, 2009.

[50] R. C. Willson, S. Gulkis, M. Janssen, H. S. Hudson, and G. A. Chapman, "Observations of solar irradiance variability," *Sciences*, vol. 211, no. 4483, pp. 700–702, 1981.

[51] P. Foukal and J. Lean, "The influence of faculae on total solar irradiance and luminosity," *The Astrophysical Journa*, vol. 302, pp. 826–835, 1986.

[52] H. C. Spruit, *Theory of Luminosity and Radius Variations, The Sun in Time*, University of Arizona Press, Tucson, AZ, USA, 1991.

[53] K. L. Yeo, N. A. Krivova, and S. K. Solanki, "Solar cycle variation in solar irradiance," *Space Science Reviews*, vol. 186, no. 1-4, pp. 137–167, 2014.

[54] N. A. Schwadron, L. A. Fisk, and T. H. Zurbuchen, "Elemental fractionation in the slow solar wind," *The Astrophysical Journal* , vol. 521, no. 2, pp. 859–867, 1999.

[55] M. Rempel and R. Schlichenmaier, "Sunspot modeling: from simplified models to radiative MHD simulations," *Living Reviews in Solar Physics*, vol. 8, no. 3, 60 pages, 2011.

[56] K. J. Li, J. C. Xu, X. H. Liu, P. X. Gao, and L. S. Zhan, "Periodicity of total solar irradiance," *Solar Physics*, vol. 267, pp. 295–303, 2010.

[57] A. Lagg, S. K. Solanki, T. L. Riethmüller et al., "Fully resolved quiet-sun magnetic flux tube observed with the sunrise/imax instrument," *The Astrophysical Journal*, vol. 723, no. 2, pp. L164–L168, 2010.

[58] J. S. Almeida, I. Márquez, J. A. Bonet, I. D. Cerdeña, and R. Muller, "Bright points in the internetwork quiet sun," *The Astrophysical Journal*, vol. 609, no. 2, pp. L91–L94, 2004.

[59] T. L. Riethmüller, S. K. Solanki, S. V. Berdyugina et al., "Comparison of solar photospheric bright points between Sunrise observations and MHD simulations," *Astronomy & Astrophysics*, vol. 568, pp. A13–23, 2014.

[60] H. C. Spruit, "Pressure equilibrium and energy balance of small photospheric fluxtubes," *Solar Physics*, vol. 50, no. 2, pp. 269–295, 1976.

[61] H. C. Spruit and C. Zwaan, "The size dependence of contrasts and numbers of small magnetic flux tubes in an active region," *Solar Physics*, vol. 70, no. 2, pp. 207–228, 1981.

[62] A. Vögler, S. Shelyag, M. Schüssler, F. Cattaneo, T. Emonet, and T. Linde, "Simulations of magneto-convection in the solar photosphere. equations, methods, and results of the MURaM code," *Astronomy & Astrophysics*, vol. 429, no. 1, pp. 335–351, 2005.